



UNIVERSITAT POLITÈCNICA  
DE CATALUNYA  
BARCELONATECH

# UPCommons

## Portal del coneixement obert de la UPC

<http://upcommons.upc.edu/e-prints>

---

This is the peer reviewed version of the following article:

Garcia-Valles, M., Alfonso, P., Arancibia, J.R.H. et al. J Therm Anal Calorim (2016) 125: 673. doi:10.1007/s10973-015-5161-4

The final publication is available at Springer via:

<http://link.springer.com/article/10.1007/s10973-015-5161-4>

---

URL d'aquest document a UPCommons E-prints:

<http://hdl.handle.net/2117/90928>

Dear Author,

Here are the proofs of your article.

- You can submit your corrections **online**, via **e-mail** or by **fax**.
- For **online** submission please insert your corrections in the online correction form. Always indicate the line number to which the correction refers.
- You can also insert your corrections in the proof PDF and **email** the annotated PDF.
- For fax submission, please ensure that your corrections are clearly legible. Use a fine black pen and write the correction in the margin, not too close to the edge of the page.
- Remember to note the **journal title**, **article number**, and **your name** when sending your response via e-mail or fax.
- **Check** the metadata sheet to make sure that the header information, especially author names and the corresponding affiliations are correctly shown.
- **Check** the questions that may have arisen during copy editing and insert your answers/ corrections.
- **Check** that the text is complete and that all figures, tables and their legends are included. Also check the accuracy of special characters, equations, and electronic supplementary material if applicable. If necessary refer to the *Edited manuscript*.
- The publication of inaccurate data such as dosages and units can have serious consequences. Please take particular care that all such details are correct.
- Please **do not** make changes that involve only matters of style. We have generally introduced forms that follow the journal's style. Substantial changes in content, e.g., new results, corrected values, title and authorship are not allowed without the approval of the responsible editor. In such a case, please contact the Editorial Office and return his/her consent together with the proof.
- If we do not receive your corrections **within 48 hours**, we will send you a reminder.
- Your article will be published **Online First** approximately one week after receipt of your corrected proofs. This is the **official first publication** citable with the DOI. **Further changes are, therefore, not possible.**
- The **printed version** will follow in a forthcoming issue.

#### **Please note**

After online publication, subscribers (personal/institutional) to this journal will have access to the complete article via the DOI using the URL: [http://dx.doi.org/\[DOI\]](http://dx.doi.org/[DOI]).

If you would like to know when your article has been published online, take advantage of our free alert service. For registration and further information go to: <http://www.link.springer.com>.

Due to the electronic nature of the procedure, the manuscript and the original figures will only be returned to you on special request. When you return your corrections, please inform us if you would like to have these documents returned.

# Metadata of the article that will be visualized in OnlineFirst

ArticleTitle	Mineralogical and thermal characterization of borate minerals from Rio Grande deposit, Uyuni (Bolivia)	
Article Sub-Title		
Article CopyRight	Akadémiai Kiadó, Budapest, Hungary (This will be the copyright line in the final PDF)	
Journal Name	Journal of Thermal Analysis and Calorimetry	
Corresponding Author	Family Name	<b>Garcia-Valles</b>
	Particle	
	Given Name	<b>M.</b>
	Suffix	
	Division	Dept. Cristallografia, Mineralogia i Dip. Minerals, Fac. Geologia
	Organization	Universitat de Barcelona
	Address	c/ Martí i Franquès, s/n, Barcelona, 08028, Spain
	Email	maitegarciavalles@ub.edu
Author	Family Name	<b>Alfonso</b>
	Particle	
	Given Name	<b>P.</b>
	Suffix	
	Division	Dept. de Enginyeria Minera i Recursos Naturals
	Organization	Universitat Politècnica de Catalunya
	Address	Avd. de les Bases de Manresa. 61-73, Manresa, 08242, Spain
	Email	
Author	Family Name	<b>Arancibia</b>
	Particle	
	Given Name	<b>J. R. H.</b>
	Suffix	
	Division	Dept. de Ingeniería Química
	Organization	Universidad Técnica de Oruro
	Address	C/ 6 de Octubre-Cochabamba, Oruro, Bolivia
	Email	
Author	Family Name	<b>Martínez</b>
	Particle	
	Given Name	<b>S.</b>
	Suffix	
	Division	Dept. Cristallografia, Mineralogia i Dip. Minerals, Fac. Geologia
	Organization	Universitat de Barcelona
	Address	c/ Martí i Franquès, s/n, Barcelona, 08028, Spain
	Email	
Author	Family Name	<b>Parcerisa</b>
	Particle	
	Given Name	<b>D.</b>

Suffix  
Division Dept. de Enginyeria Minera i Recursos Naturals  
Organization Universitat Politècnica de Catalunya  
Address Avd. de les Bases de Manresa. 61-73, Manresa, 08242, Spain  
Email

---

Schedule  
Received 21 July 2015  
Revised  
Accepted 12 November 2015

---

Abstract Large volumes of borate resources exist in Bolivia, with the most important being the Rio Grande deposit, located close to the Salar of Uyuni. Here, borates occur in beds and lenses of variable thickness. A mineralogical and thermal characterization of borates from the Rio Grande was made using XRD, FTIR, SEM and DTA–TG. The deposit is mainly composed of  $B_2O_3$ , CaO and  $Na_2O$ , with minor contents of MgO and  $K_2O$ . Some outcrops are constituted by pure ulexite aggregates ( $NaCaB_5O_6(OH)_6 \cdot 5H_2O$ ) of fibrous morphology; in other cases, gypsum, calcite and halite also are present. The thermal decomposition of ulexite begins at 70 °C and proceeds up to ~550 °C; this decomposition is attributed to dehydration and dehydroxylation processes in three steps: at 115, 150–300 and 300–550 °C. The last weight loss of 1–5 % at 800 °C is due to the removal of  $Cl_2$  from the decomposition of halite. DTA shows two endothermic events related to the removal of water; in the first,  $NaCaB_5O_6(OH)_6 \cdot 5H_2O$  evolved from  $NaCaB_5O_6(OH)_6 \cdot 3H_2O$ , at 108–116 °C; in the second,  $NaCaB_5O_6(OH)_6$  is formed at 180–185 °C and  $NaCaB_5O_9$  (amorphous) is formed at 300–550 °C. The exothermic peak (658–720 °C) is related to the crystallization of  $NaCaB_5O_9$ . A small endothermic peak appears due to the halite melting. Later, another endothermic event (821–877 °C) appears, which is related to the decomposition of  $NaCaB_5O_9$  into a crystalline phase of  $CaB_2O_4$  and amorphous  $NaB_3O_5$ . The XRD pattern evidences that, at 1050 °C,  $CaB_2O_4$  still remains in the crystalline state.

---

Keywords (separated by '-') Borate minerals - Ulexite - Thermal evolution - DTA–TG - XRD - FTIR

---

Footnote Information

---

7

## 3 Mineralogical and thermal characterization of borate minerals 4 from Rio Grande deposit, Uyuni (Bolivia)

5 M. Garcia-Valles<sup>1</sup> · P. Alfonso<sup>2</sup> · J. R. H. Arancibia<sup>3</sup> · S. Martínez<sup>1</sup> ·  
6 D. Parcerisa<sup>2</sup>

7 Received: 21 July 2015 / Accepted: 12 November 2015  
8 © Akadémiai Kiadó, Budapest, Hungary 2015

9 **Abstract** Large volumes of borate resources exist in  
10 Bolivia, with the most important being the Rio Grande  
11 deposit, located close to the Salar of Uyuni. Here, borates  
12 occur in beds and lenses of variable thickness. A miner-  
13 alogical and thermal characterization of borates from the  
14 Rio Grande was made using XRD, FTIR, SEM and DTA–  
15 TG. The deposit is mainly composed of B<sub>2</sub>O<sub>3</sub>, CaO and  
16 Na<sub>2</sub>O, with minor contents of MgO and K<sub>2</sub>O. Some out-  
17 crops are constituted by pure ulexite aggregates (NaCaB<sub>5</sub>-  
18 O<sub>6</sub>(OH)<sub>6</sub>·5H<sub>2</sub>O) of fibrous morphology; in other cases,  
19 gypsum, calcite and halite also are present. The thermal  
20 decomposition of ulexite begins at 70 °C and proceeds up  
21 to ~550 °C; this decomposition is attributed to dehydra-  
22 tion and dehydroxylation processes in three steps: at 115,  
23 150–300 and 300–550 °C. The last weight loss of 1–5 % at  
24 800 °C is due to the removal of Cl<sub>2</sub> from the decomposi-  
25 tion of halite. DTA shows two endothermic events related  
26 to the removal of water; in the first, NaCaB<sub>5</sub>O<sub>6</sub>(OH)<sub>6</sub>·5H<sub>2</sub>O  
27 evolved from NaCaB<sub>5</sub>O<sub>6</sub>(OH)<sub>6</sub>·3H<sub>2</sub>O, at 108–116 °C; in  
28 the second, NaCaB<sub>5</sub>O<sub>6</sub>(OH)<sub>6</sub> is formed at 180–185 °C and  
29 NaCaB<sub>5</sub>O<sub>9</sub> (amorphous) is formed at 300–550 °C. The  
30 exothermic peak (658–720 °C) is related to the crystal-  
31 lization of NaCaB<sub>5</sub>O<sub>9</sub>. A small endothermic peak appears

due to the halite melting. Later, another endothermic event 32  
(821–877 °C) appears, which is related to the decomposi- 33  
tion of NaCaB<sub>5</sub>O<sub>9</sub> into a crystalline phase of CaB<sub>2</sub>O<sub>4</sub> and 34  
amorphous NaB<sub>3</sub>O<sub>5</sub>. The XRD pattern evidences that, at 35  
1050 °C, CaB<sub>2</sub>O<sub>4</sub> still remains in the crystalline state. 36

**Keywords** Borate minerals · Ulexite · Thermal 38  
evolution · DTA–TG · XRD · FTIR 39

### 40 Introduction 40

Bolivia has large volumes of borate resources, the most 41  
important being the playa -lake type deposit of the Rio 42  
Grande, which has total reserves estimated at approxi- 43  
mately 1.6 Mt of boron [1, 2]. This deposit comprises an 44  
area of approximately 50 km<sup>2</sup> located close to the southern 45  
part of the Salar of Uyuni in the contact between fluvio- 46  
deltaic and lacustrine sediments in the Río Grande de Lipez 47  
delta. The deposit is being exploited, and borates are 48  
commercialized after a natural dehydration process, calci- 49  
nation and grinding. 50

Borates are classified as critical materials by the Euro- 51  
pean Union [3]. Borate minerals are the main source of 52  
boron and have a multitude of industrial applications [4]. In 53  
addition to classical applications of boron in glass, 54  
ceramics, fertilizers, special alloys, aeronautics, nuclear, 55  
military vehicles, fuels, electronics and communications, 56  
new uses appear daily, such as for polymeric materials [5] 57  
and for imparting halogen-free flame-retardant properties 58  
to cellulose-based materials [6]. Ca-, Na-borate minerals 59  
are mainly applied for making fiberglass, but are also used 60  
for ceramics and ceramic glazes [7, 8]. Other applications 61  
reported for Ca-rich borates include nuclear technology [9] 62  
and the refractory industry. 63

A1 ✉ M. Garcia-Valles  
A2 maitegarciavalles@ub.edu

A3 <sup>1</sup> Dept. Cristallografia, Mineralogia i Dip. Minerals, Fac.  
A4 Geologia, Universitat de Barcelona, c/ Martí i Franquès,  
A5 s/n, 08028 Barcelona, Spain

A6 <sup>2</sup> Dept. de Enginyeria Minera i Recursos Naturals, Universitat  
A7 Politècnica de Catalunya, Avd. de les Bases de Manresa.  
A8 61-73, 08242 Manresa, Spain

A9 <sup>3</sup> Dept. de Ingeniería Química, Universidad Técnica de Oruro,  
A10 C/ 6 de Octubre-Cochabamba, Oruro, Bolivia

64 The industrial uses of borate minerals greatly depend  
65 upon its thermal properties. Therefore, to recommend the  
66 optimal application of borate minerals, knowing the ther-  
67 mal properties is important.

68 Numerous studies on the thermal properties of borate  
69 minerals have been reported; some of them use mixtures of  
70 different borate minerals [10, 11] or a specific mineral,  
71 such as ulexite [12–14].

72 In this paper, we present a mineralogical and thermal  
73 characterization of borates from the Rio Grande deposit in  
74 Bolivia with special emphasis on the mineralogy of the  
75 different events during thermal treatment.

## 76 Geological setting

77 The Bolivian Altiplano is a major basin filled with thick  
78 sequences of continental sediments of Cretaceous to Ter-  
79 tiary age [15]. In the quaternary, endorheic basins of the  
80 Altiplano were occupied by large lakes, which progres-  
81 sively reduced its size due to intense evaporation and low  
82 precipitation that occurred in the region during the last  
83 10,000 years, giving rise to the salt lakes and salars, such  
84 as Poopó, Uyuni and Coipasa, in the Central Altiplano.

85 The western and southern areas of the Altiplano were  
86 strongly affected by an intense volcanic activity from the  
87 Oligocene to the Quaternary. Volcanic rocks range from  
88 andesites to rhyodacites with abundant ignimbrites [2],  
89 which are considered to be the source of lithium and boron  
90 of the salars and nearby evaporitic deposits [16].

91 More than 40 borate deposits occur in the Andean belt  
92 related to salars [17]. The Rio Grande borate deposit occurs  
93 in the southern region of the salar of Uyuni, the largest on

94 Earth, and is composed of deltaic-lacustrine sediments in  
95 contact with the salt crust (Fig. 1) [18]. Borates precipi-  
96 tated by capillary rise and subsequent evaporation of the  
97 groundwater. Silty sediments occur in contact with the  
98 water of the salar; groundwater rises due to porosity and  
99 drops evaporate when they reach the surface and the dis-  
100 solved components precipitate when they come into con-  
101 tact with the water layer. The borate deposit is not in the  
102 area of higher concentrations of Li, K and B, but rather  
103 further to the south. Ulexite precipitation is controlled by  
104 the concentrations of Ca, Na and B in the brine [2].

105 In this deposit, borates occur in beds and lenses of  
106 variable thickness, from 0.5 to 5 m. In the western region  
107 of the deposit, the lenses outcrop in small reliefs of several  
108 cm. In the eastern area of the deposit, the bed of borates is  
109 present at a depth up to 2 m below the clay level. Borate  
110 minerals form brittle nodules with a cotton-ball texture  
111 near the surface interbedded within the fluvial-deltaic  
112 sediment layers constituted by gypsum, clays and sands.  
113 The clays are mainly montmorillonite, illite and kaolinite  
114 [2].

## 115 Materials and methods

116 Seven samples of borate minerals were obtained from  
117 different outcrops in the Rio Grande deposit along 4.5 km,  
118 and all the samples were collected from the natural  
119 occurrence in the deposit (Fig. 1).

120 The chemical composition was determined by induc-  
121 tively coupled plasma mass spectrometry (ICP-MS) using  
122 an Agilent 7500ce OPTIMA 3200RL ICP-MS spectrome-  
123 ter with a reaction cell.

124 The mineralogy of the natural and thermally treated  
125 samples was determined by X-ray diffraction (XRD). The  
126 spectra were obtained from powdered samples (particles  
127 under 45  $\mu\text{m}$ ) in a Bragg–Brentano PANalytical X'Pert  
128 Diffractometer system (graphite monochromator, automatic  
129 gap,  $K\alpha$  radiation of Cu at  $\lambda = 1.54061 \text{ \AA}$ , powered at  
130 45 kV, 40 mA, scanning range 4–100° with a 0.017°  $2\theta$  step  
131 scan and a 50-s measuring time). The identification and  
132 semiquantitative evaluation of phases were conducted using  
133 a PANalytical X'Pert HighScore software. Chemical  
134 bonds in the borate structure were also characterized by  
135 Fourier transform infrared spectroscopy (FTIR). Vibra-  
136 tional spectra were obtained in the 400–4000  $\text{cm}^{-1}$  range  
137 using a Perkin Elmer Frontier FTIR spectrophotometer.  
138 Original borates textures were observed by scanning elec-  
139 tron microscopy (SEM) using a Quanta 200 FEI, XTE  
140 325/D8395 environmental scanning electron microscope.

141 Thermal evolution of each mineral phase and the nature  
142 and mechanisms of thermal decomposition were obtained  
143 by differential thermal analysis and thermogravimetry



Fig. 1 Location of the Rio Grande borate deposit

(DTA–TG) using a Netzsch equipment (STA 409C model). Analyses were conducted under N<sub>2</sub> inert atmosphere at 80 ml min<sup>-1</sup> constant flow ratio, using Pt crucible, temperature range 25–1200 °C with a linear rate of temperature gradient set to 10 °C min<sup>-1</sup>. According to DTA–TG results, to determine the mineral evolution with temperature, the heat treatment temperatures were established with a setting time of half an hour, and subsequent analysis by XRD was performed. The heat treatment ranged from 550 to 1050 °C.

## 154 Results and discussion

### 155 Chemical composition

The chemical composition of the Rio Grande borate deposit is presented in Table 1. The main components are B<sub>2</sub>O<sub>3</sub>, between 36.21 and 42.60 wt%, CaO, between 12.70 and 13.74 wt%, and Na<sub>2</sub>O, from 7.61 to 13.04 wt%, which suggests that borate minerals constitute the main mineral. In some outcrops, the chemical composition is close to that of pure ulexite (NaCaB<sub>5</sub>·5H<sub>2</sub>O) with 42.95 % B<sub>2</sub>O<sub>3</sub>. In other cases, Na is relatively high. Other elements occur in minor amounts; for example, MgO is up to 1.5 wt%, and K<sub>2</sub>O up to 0.67 wt%. Fe, Al, Sr and other elements occur in trace amounts.

### 167 Mineralogy

In accordance with the data obtained by the chemical analyses, the XRD patterns show that ulexite (NaCaB<sub>5</sub>O<sub>6</sub>(OH)<sub>6</sub>·5H<sub>2</sub>O) is the main mineral phase in the borate deposit. Among the wide range of over 160 species of borate minerals, ulexite is one of the most economically

important [19]. In some cases, it is the only mineral present. However, in most outcrops, other evaporite minerals, mainly halite (NaCl) and gypsum (CaSO<sub>4</sub>·2H<sub>2</sub>O), also occur. Figure 2 shows a representative XRD pattern from the Rio Grande deposit.

Ulexite occurs as crystalline aggregates with morphology of elongated fibers oriented parallel to each other along [001], greater than 100 microns in length (Fig. 3a). Equant sodium chloride crystals giving rise to dissolution phantoms are located among ulexite fibers (Fig. 3b). Gypsum also forms euhedral crystals up to several cm in size (Fig. 3c).

Infrared spectroscopy, FTIR (Fig. 4), was used to confirm the mineral phases determined by XRD. Ulexite from Rio Grande shows peaks in different spectral ranges. In general, the first bands correspond to water stretching vibrations and the other bands are simply defined as rhombohedral and tetrahedral borate bending modes. A broad band with several overlapping peaks is displayed between the 3600 and 3150 cm<sup>-1</sup> region assigned to the stretching vibration mode of the O–H group. The bands at 1667 and 1632 cm<sup>-1</sup> are assigned to the bending mode of H–O–H and free water, respectively. The asymmetric stretching of three-coordinate boron (BO<sub>3</sub>) was observed in the range of 1479–1240 cm<sup>-1</sup>. The bands between 1240 and 1155 cm<sup>-1</sup> correspond to B–O–H in plane bending modes. An asymmetric stretching mode of B–O in BO<sub>4</sub> was observed between 1027 and 959 cm<sup>-1</sup>. The bands at 887–839 and 756 cm<sup>-1</sup> are assigned to the asymmetric and symmetric stretching of B–O in BO<sub>4</sub>, respectively. The band at 663 cm<sup>-1</sup> is the bending to the symmetric stretching mode of three-coordinate boron. The final peaks, located at 561–546 cm<sup>-1</sup>, are assigned to the bending modes of BO<sub>4</sub> groups [14].

### 207 Thermal evolution

Thermal decomposition of borates is a complex mechanism which involves dehydration, polymorphic transition and

**Table 1** Chemical composition of the borates from the Rio Grande deposit

wt%	RG-1a	RG-1b	RG-2	RG-3	RG-4	RG-5	RG-7
CaO	13.38	13.74	11.82	13.83	12.90	13.59	12.70
MgO	0.67	0.42	1.46	0.13	0.69	0.94	1.08
Na <sub>2</sub> O	9.71	8.36	13.04	7.61	9.95	9.33	10.90
K <sub>2</sub> O	0.22	0.16	0.67	0.02	0.25	0.28	0.41
B <sub>2</sub> O <sub>3</sub>	41.13	40.99	36.21	42.60	39.34	41.65	38.91
Traces/ppm							
Sr	151	786	230	247	441	140	149
Mn	1.51	16.6	2.23	5.90	8.74	3.17	2.40
Al	16.6	676	10.6	200	87.6	12.1	17.0
Fe	9.39	376	6.75	105	72.7	18.7	18.3
Ti	–	28.1	–	9.52	–	–	–
As	1.90	8.20	2.00	4.30	9.30	3.40	1.60

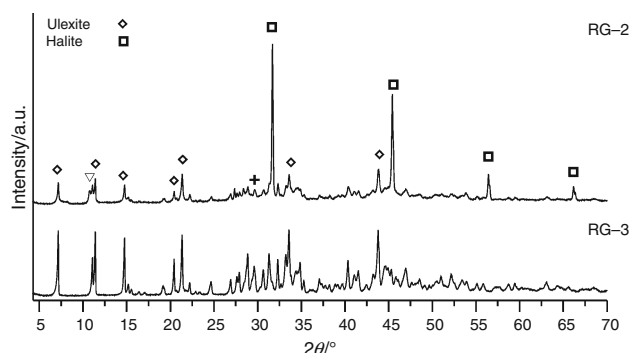


**Fig. 2** XRD patterns of two representative samples. RG-2 is the halite rich sample, and RG-3 is nearly pure ulexite

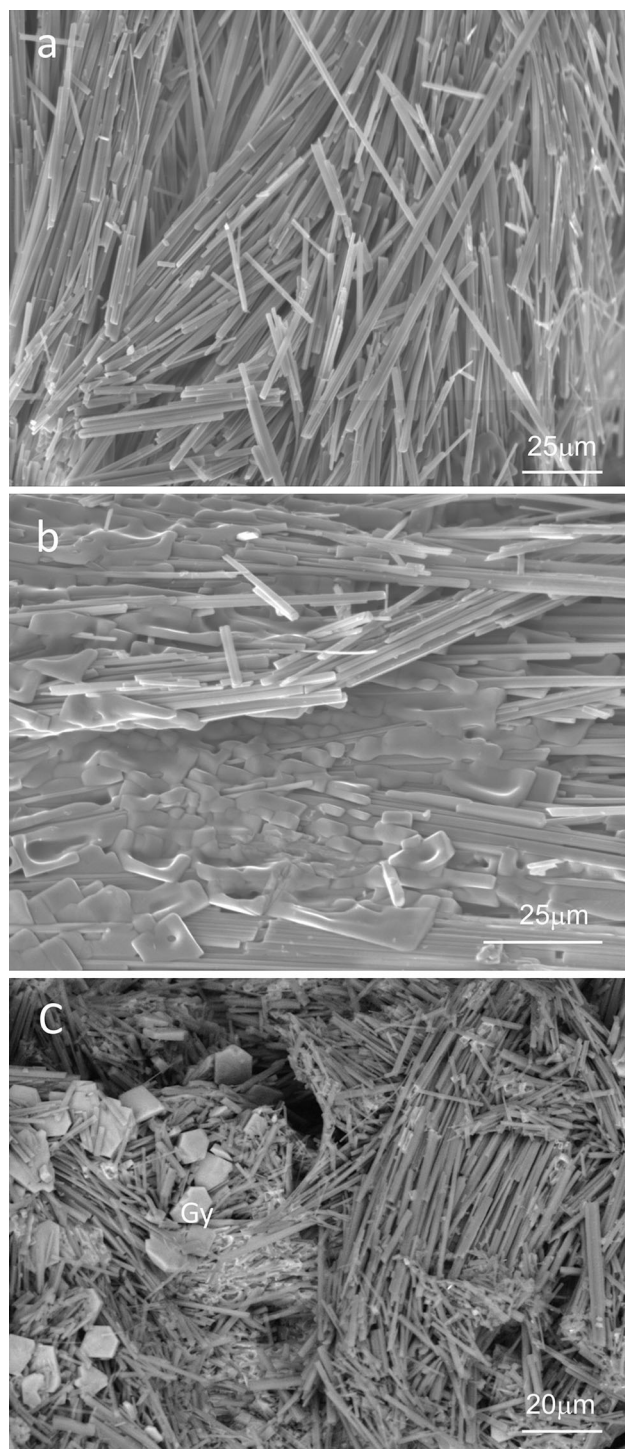


**Fig. 3** SEM images of borates from Rio Grande, **a** fibrous ulexite, **b** ulexite with deliquescent halite, **c** ulexite accompanied with euhedral gypsum crystals

210 solid phase transformation [20]. In the case of ulexite, the  
 211 decomposition process develops in the different stages  
 212 shown in the DTA–TG curves (Figs. 5, 6). Decomposition

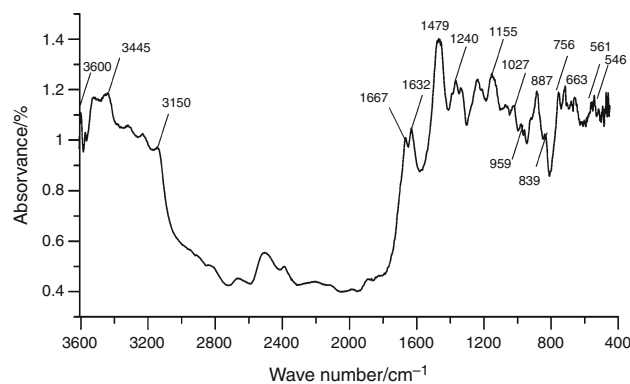


**Fig. 4** FTIR spectrum of ulexite from Rio Grande salar

begins at approximately 70 °C and proceeds up to ~550 °C; these temperatures can be attributed to dehydration and dehydroxylation processes [21–23].

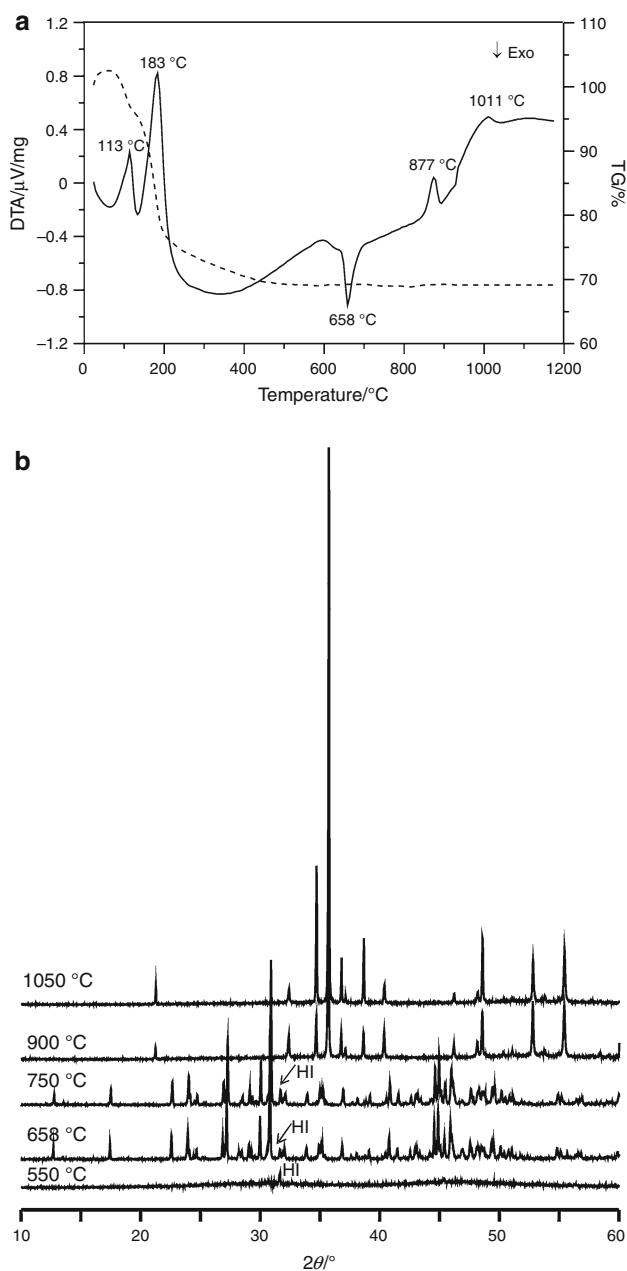
The TG curves indicate that these processes present a weight loss in three steps (Table 2); 3.4–5.7 wt% of mass loss is attributed to the release of two molecules of crystal water at approximately 115 °C (1). This loss is lower than the expected for the loss of two molecules of water, which is likely due to sample manipulation. The second loss, 11–14.9 wt%, between 150 and 300 °C, is attributed to the removal of the three molecules of crystal water (2), and the last, 11–16.2 wt% of mass loss is due the release of another three molecules of crystal water, between 300 and 550 °C, that corresponds to dehydroxylation of ulexite (3). Sener et al. [20] indicate that in the first stage of dehydration 1.5 of water molecules is released at approximately 118 °C. During the second stage, between 118 and 260 °C, 0.5 in 2.5 water molecules is lost in two endothermic events. Later, the OH groups are liberated as three water molecules. However, Seyhun et al. [22] attributed the loss of three water molecules to the first event and two molecules to the second event.

Figure 5 shows the TG curve of the pure ulexite sample; in this case, the global weight loss of 33.5 % corresponds to eight water molecules, similar to the results obtained in other studies of ulexite [14, 22].

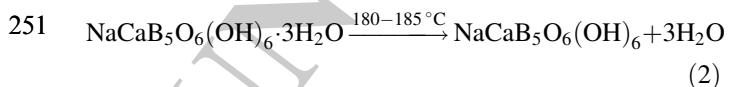
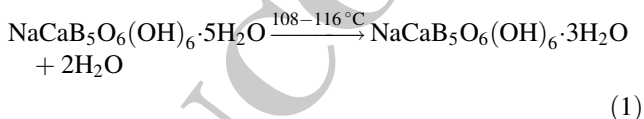
All samples, with the exception of RG-3, exhibit a final weight loss of 1–5 % at 800 °C due to the removal of chlorine from the decomposition of the sodium chloride present in the samples.

The transformations were controlled by XRD analysis at temperature intervals (Fig. 5). In the DTA analysis, four endothermic and one exothermic events are observed. The first two are related to the removal of the crystal water shown in the TG measurements at the interval of 108–116 °C (1) and 180–185 °C (2) according to the following reactions:





**Fig. 5** Pure ulexite (RG-3) **a** DTA–TG curves and **b** sequential XRD patterns showing the new phases formed at each treatment temperature



The next reaction, corresponding to the loss of OH groups, did not explicitly show an endothermic phenomenon due to the slow process (3):

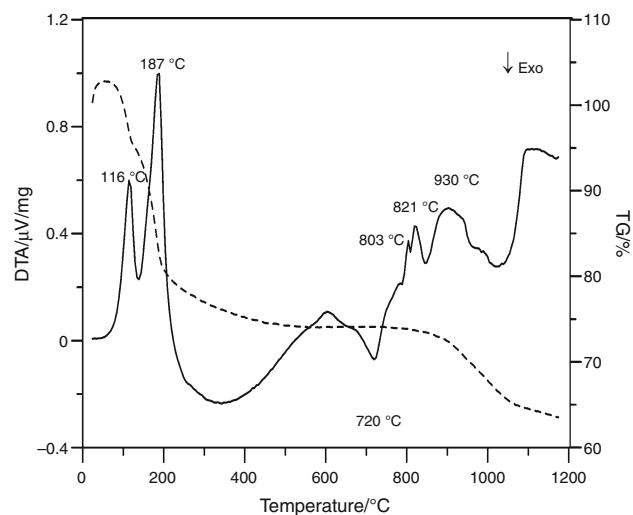
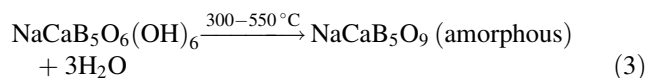


**Fig. 6** DTA–TG curves corresponding to a borate sample rich in halite (RG-7)

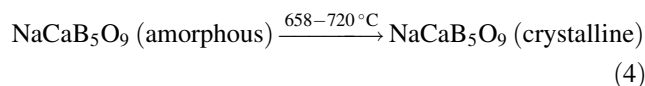
**Table 2** Mass loss (wt%) for different ranges of temperature of the Rio Grande borate deposit

Sample	Range of temperature/°C		
	70–115	150–300	300–550
RG-1a	3.4	12.7	13.6
RG-1b	3.4	14.1	13.4
RG-2	3.4	11.0	11.0
RG-3	4.0	14.4	14.8
RG-4	3.7	12.1	12.8
RG-5	3.6	14.1	14.7
RG-7	5.7	14.9	16.1



Ulexite releases eight mol of water in the range of 70–550 °C, and it changes to the  $\text{CaNaB}_5\text{O}_9$  form (amorphous borate phase). The XRD patterns (Fig. 2) show the amorphous structure of the borates at 550 °C. At this temperature, the only crystalline phase present is halite.

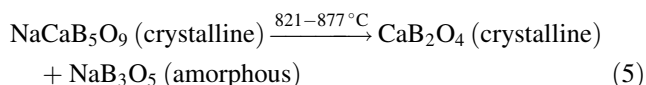
The exothermic peak at the interval of 658–720 °C is related to the crystallization process of the amorphous  $\text{NaCaB}_5\text{O}_9$  given as follows (4):



When the sample is rich in halite, a new endothermic peak appears near 803 °C due to halite melting (Fig. 6). This temperature increases with the halite content.

The endothermic peak at the interval of 821–877 °C (Fig. 5) is related to the decomposition of  $\text{NaCaB}_5\text{O}_9$  (5).

271 Similar values have been reported for pure ulexite samples  
272 [14, 20]. The temperature of this endothermic peak  
273 decreases when the halite content increases in the borate  
274 sample, up to 821 °C in a sample with 23 wt% of halite  
275 (Fig. 6).



277 The thermal evolution of the Rio Grande borates pro-  
278 ceeds as mentioned for other ulexite occurrences [20]. On  
279 the contrary, other authors, for example Stoch and  
280 Waclawska [21], attributed an endothermic peak at 854 °C  
281 to the melting temperature of  $\text{CaB}_2\text{O}_4$ . The crystallization  
282 of amorphous  $\text{NaCaB}_5\text{O}_9$  directly to  $\text{CaB}_2\text{O}_4$  and amorphous  
283  $\text{NaB}_3\text{O}_5$  was also previously suggested.

284 The melting of the previous phases was reported at  
285 862 °C [14]; Gazualla [24] determined that  $\text{NaB}_3\text{O}_5$  melted  
286 at 873 °C and  $\text{CaB}_2\text{O}_4$  melted at 1014 °C. Nevertheless, in  
287 the present work the experimental temperature reached  
288 1050 °C, and the XRD patterns indicated the presence of  
289 crystalline  $\text{CaB}_2\text{O}_4$  at least up to 1050 °C (Fig. 5). In  
290 addition, in the DTA diagram, obtained up to 1200 °C, any  
291 endothermic peak characteristic of melting is observed.

292 The endothermic temperature related to the formation of  
293  $\text{CaB}_2\text{O}_4$  depends on the alkalis and boron contents. The  
294 temperature of  $\text{NaCaB}_5\text{O}_9$  decomposition increases with an  
295 increase in the boron ratio in tetrahedral coordination to  
296 achieve a maximum value, and then, it decreases again  
297 (Fig. 7). This point coincides with the boric anomaly,

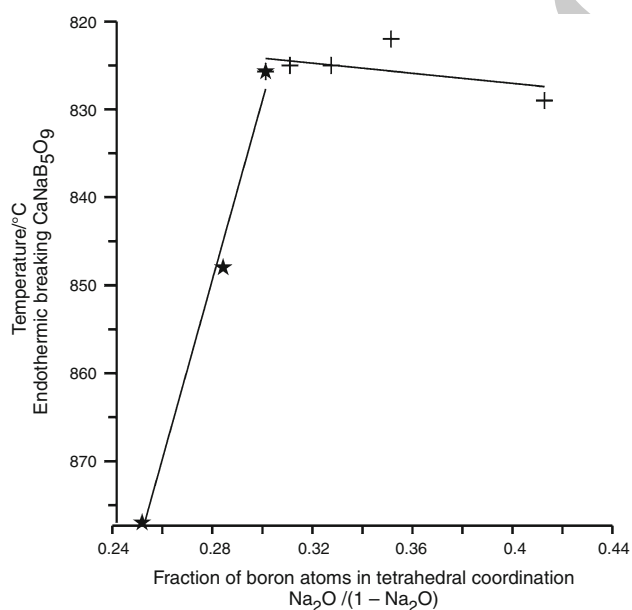


Fig. 7 Representation of the temperature of  $\text{NaCaB}_5\text{O}_9$  decomposition as a function of the fraction of boron atoms in tetrahedral coordination

298 which occurs at approximately 30 % molar in  $\text{Na}_2\text{O}$ . This  
299 reaction is produced without mass loss (Fig. 5).

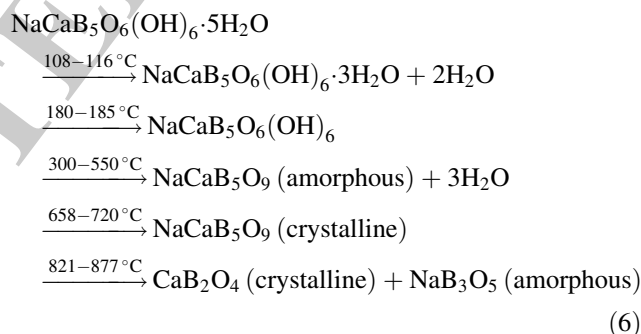
300 The crystal structure of  $\text{NaCaB}_5\text{O}_6(\text{OH})_6 \cdot 5\text{H}_2\text{O}$  has  
301 three borate tetrahedra and two borate triangles [25]. When  
302 the structure is heated, water is released and  $\text{NaCaB}_5\text{O}_9$  is  
303 formed, and the new structure is composed of two borate  
304 tetrahedra and three borate triangles [26]. Finally, when the  
305 structure decomposes into  $\text{CaB}_2\text{O}_4 + \text{NaB}_3\text{O}_5$ , in the Ca-  
306 borate, crystalline, all the boron groups are in a plane tri-  
307 angular coordination [27].

308 The borate crystal structure was destroyed by dehydra-  
309 tion, and an amorphous structure was formed; however,  
310 under heat, the crystalline structure is formed again [28].  
311 Then, with the temperature increase, ulexite dehydration  
312 causes changes in the stable phases and, thus, in the ratio of  
313 tetrahedral and triangular boron coordination.

## 314 Conclusions

315 The Rio Grande borate deposit is mainly comprised of  
316 ulexite, as well as occasional other evaporite minerals, such  
317 as halite and minor gypsum.

318 The thermal evolution of ulexite from the studied  
319 deposit is shown in the next sequence (6):



321 Regarding the heat treatment of borates, this study has  
322 shown that, at 1050 °C, the  $\text{CaB}_2\text{O}_4$  crystalline phase is  
323 still present; therefore, the melting temperature will be  
324 above this temperature.

325 The decomposition temperature of  $\text{NaCaB}_5\text{O}_9$  is influ-  
326 enced by the halite content. This temperature decreases  
327 when the halite content increases in the sample; however,  
328 the halite melting temperature rises with the halite content.

329 Halite should be removed from borates of the Rio  
330 Grande deposit to improve the industrial treatment of  
331 borates.

332 **Acknowledgements** This research was financed by the Project  
333 AECID: A3/042750/11 and the Consolidated Group for Research of  
334 Mineral Resources, 2014 SGR-1661) and by the Bosch i Gimpera  
335 Foundation Project 307466. The authors would like to thank the staff of  
336 the Centres Científics i Tecnològics of the University of Barcelona  
337 (CCiTUB) for their technical support.

## References

- 339 1. Risacher F. Origine des concentrations extremes en bore et en  
340 lithium dans les saumures de l'Altiplano bolivien. CR Acad Sci  
341 Paris Sér. 1984;2(299):701–6.
- 342 2. Risacher F, Fritz B. Quaternary geochemical evolution of the  
343 salars of Uyuni and Coipasa, Central Altiplano, Bolivia. Chem  
344 Geol. 1991;90:211–31.
- 345 3. European Union. Report on critical raw materials for the EU 2014;  
346 pp. 41.
- 347 4. Woods WG. An introduction to boron: history, sources, uses, and  
348 chemistry. Environ Health Perspect. 1994;102:5–11.
- 349 5. Nazari A, Maghsoudpour A, Sanjayan JG. Characteristics of  
350 boroaluminosilicate geopolymers. Constr Build Mat. 2014;70:  
351 262–8.
- 352 6. Dogan M. Thermal stability and flame retardancy of guanidinium  
353 and imidazolium borate finished cotton fabrics. J Therm Anal  
354 Calorim. 2014;118:93–8.
- 355 7. Stefanov S. Applications of borate compounds for the preparation  
356 of ceramic glazes. Glass Technol. 2000;41:193.
- 357 8. Christogerou A, Kavas T, Pontikes Y, Koyas S, Tabak Y,  
358 Angelopoulos GN. Use of boron wastes in the production of  
359 heavy clay ceramics. Ceram Int. 2009;35:447–52.
- 360 9. Akan M, Doğan M. Dissolution kinetics of colemanite in oxalic  
361 acid solutions. Chem Eng Process. 2004;43:867–72.
- 362 10. Waclawska I. Controlled rate thermal analysis of hydrated  
363 borates. J Thermal Anal. 1998;53:519–32.
- 364 11. Derun EM, Kipçak AS. Characterization of some boron minerals  
365 against neutron shielding and 12 year performance of neutron  
366 permeability. J Radioanal Nucl Chem. 2012;291:871–8.
- 367 12. Ruoyu C, Jun L, Shuping X, Shiyang G. Thermochemistry of  
368 ulexite. Thermochim Acta. 1997;306:1–5.
- 369 13. Correcher V, Garcia-Guinea J, Valle-Fuentes FJ. Preliminary  
370 study of the thermally stimulated blue luminescence of ulexite.  
371 J Therm Anal Calorim. 2006;83:439–44.
- 372 14. Piskin MB. Investigation of sodium borohydride production  
373 process: “Ulexite mineral as a boron source”. Int J Hydrogen  
374 Energy. 2009;34:4773–9.
- 375 15. Risacher F, Fritz B. Origin of salts and brine evolution of Boli-  
376 vian and Chilean salars. Aquat Geochem Geol. 2009;15:123–57.
16. Orris GJ. Geology and mineral resources of the Altiplano and  
377 Cordillera Occidental, Bolivia: undiscovered nonmetallic depos-  
378 its. Bull US Geol Surv. 1992;1975:225–9. 379
17. Helvacı C, Alonso RN. Borate deposits of Turkey and Argentina:  
380 a summary and geological comparison. Turkish J Earth Sci.  
381 2000;9:1–27. 382
18. Marsh SP, Richter DH, Ludington S, Soria-Escalante E, Escobar-  
383 Diaz A. Geologic map of the Altiplano and Cordillera Occidental,  
384 Bolivia. In: U.S. Geological Survey and Servicio Geologico de  
385 Bolivia, Geology and mineral resources of the Altiplano and  
386 Cordillera Occidental, Bolivia: U.S. Geological Survey Bulletin;  
387 1975; 365 p. scale 1:500000. 388
19. Helvacı C, Borates. Encyclopedia Geol. 2005; pp. 510–522. **AQ4** 389
20. Şener S, Özbayoğlu G, Demirci Ş. Changes in the structure of  
390 ulexite on heating. Thermochim Acta. 2000;362:107–12. 391
21. Stoch L, Waclawska I. Thermal decomposition of hydrates  
392 borates. Thermochim Acta. 1993;215:273–9. 393
22. Kipçak AS, Derun EM, Piskin S. Characterisation and determi-  
394 nation of the neutron transmission properties of sodium–calcium  
395 and sodium borates from different regions in Turkey. J Radioanal  
396 Nucl Chem. 2014;301:175–88. 397
23. Erdoğan Y, Zeybek A, Sahin A, Demirbas A. Dehydration  
398 kinetics of howlite, ulexite, and tunellite using thermogravimetric  
399 data. Thermochim Acta. 1999;326:99–103. 400
24. Gazulla MF, Gómez MP, Orduña M, Silva G. Caracterización  
401 química, mineralógica y térmica de boratos naturales y sintéticos.  
402 Bol Soc Ceram Vidr. 2005;44:21–31. 403
25. Christ CL, Clark JR. A crystal–chemical classification of borate  
404 structures with emphasis on hydrated borates. Chem Minerals.  
405 1977;2:59–87. 406
26. Fayos J, Howie RA, Glasser FP. Structure of calcium sodium  
407 pentaborate. Acta Crystallogr C. 1985;41:1394–6. 408
27. Kirfel A. The electron density distribution in calcium metaborate,  
409 Ca(BO<sub>2</sub>)<sub>2</sub>. Acta Crystallogr. 1987;B43:333–43. 410
28. Tkachenko EA, Fedorov PP, Kuznetsov SV, Voronov VV,  
411 Lavrishchev SV, Shukshin VE. Synthesis of nanocrystalline  
412 indium orthoborate through borate rearrangement. Russian J  
413 Inorg Chem. 2005;50:681–4. 414

UNCORRECTED

Journal : **10973**

Article : **5161**

## Author Query Form

**Please ensure you fill out your response to the queries raised below and return this form along with your corrections**

Dear Author

During the process of typesetting your article, the following queries have arisen. Please check your typeset proof carefully against the queries listed below and mark the necessary changes either directly on the proof/online grid or in the 'Author's response' area provided below

Query	Details Required	Author's Response
AQ1	Please check the edit made in the sentence 'DTA shows two endothermic events ...to the crystallization of NaCaB5O9'.	
AQ2	The term 'PANAnalytical' is used inconsistently with respect to capitalization. Please suggest which occurrence to be followed consistently.	
AQ3	Please check the missing open parenthesis in the sentence 'This research was financed ...Gimpera Foundation Project 307466'.	
AQ4	Please update the complete details in Ref. [19].	